TITLE PAGE

- **TITLE**

Roles of moisture and cyclic loading in microstructures and their effects on mechanical properties for typical Chinese bituminous coals

- **Authors and affiliations**

Qiangqiang Ren [a], Yufei Zhang [a, c], Inmaculada Arauzo [b, c], Lianying Shan [a, c], Jun Xu [a, *], Yi Wang [a, c], Sheng Su [a, c], Song Hu [a, c, *], Jun Xiang [a, c]

[a] State Key Laboratory of Coal Combustion, School of Energy and Power Engineering, Huazhong University of Science and Technology, Wuhan 430074, China

[b] Department of Mechanical Engineering, University of Zaragoza, Mariano Esquillor 15, E-50018 Zaragoza, Spain

[c] China-EU Institute for Clean and Renewable Energy, Huazhong University of Science and Technology, Wuhan 430074, China

- **Corresponding authors**

State Key Laboratory of Coal Combustion, School of Energy and Power Engineering, Huazhong University of Science and Technology, Wuhan 430074, China

Tel.: +86-27-87542417, Fax: +86-27-87545526

E-mail: xujun_sklcc@hust.edu.cn (Jun Xu), husong_hust@hotmail.com (Song Hu).

Abstract:

This work aimed at studying the roles of moisture and cyclic loading in microstructures and their effects on mechanical properties for typical Chinese bituminous coals. Different relative moisture contents (100%, 75%, 50%, 25%, and 0%) for Shenmu coal (SM), Hongshaquan coal (HSQ), and Wucaiwan coal (WCW) were chosen to study the effects of moisture. The raw SM was then further selected to investigate the effects of cyclic loading. Images of coals surfaces and mechanical properties during simulated crushing process were recorded and combined to be analyzed. The results showed that the moisture possessed significant effects on coal mechanical properties, which strongly depended on their porosities. As for low porosity coal (SM), the adsorption of moisture can soften and lubricate the microstructures, weakening mechanical properties. While the drying process would destroy the microstructures and decease mechanical properties for high porosity coals (HSQ and WCW). Under the cyclic loading process, the cumulative effects of strain showed a step-up state and the first cyclic loading can typically cause biggest change of microstructures and produce the largest strain under different stress levels. Finally, a normalized quantitative relationship ($\sigma_r = -0.67D_r^2 + 1.62D_r + 0.07$) between the relative fractal dimension and relative stress was built.

Keywords: bituminous coal; moisture; cyclic loading; crushing; microstructures; mechanical properties.

1. Introduction

Coal, a key fuel, will still occupy 20% energy consumption in the world, and even over 50% in many developing countries such as China, India, South Africa, and so on as estimated by 2040 [1-3]. As it is widely known that the utilization of coal cannot be separable from the crushing process, by which higher coal conversion efficiency and lower pollutant emissions can be achieved [4]. But, the coal crushing process would consume huge quantities of energy, even about 1% of the electricity produced by coal-fired power plant [5]. Besides, coal crushing process is also an extremely complex process [6, 7]. Deeply studying the properties and mechanisms of coal crushing process is key for saving energy and efficient coal utilization.

The essence of coal crushing process is the deformation of physical structure [8, 9] and the crushing process is closely related to the mechanical properties of raw coal [8, 10]. Besides, it has been directly shown by the previous researches that the mechanical properties of coal were not only affected by the external environment such as moisture [11-12] and heating [13], but also by the internal factors such as composition [2, 14, 15] and pore structure [16, 17]. These factors either cause the change of microstructures or thus affect the mechanical properties of coal. However, the effects of some typical external factors on internal microstructures have not been fully studied yet, while the relationship between the coal microstructures and mechanical properties has not been quantitatively understood, which can assist to further reveal the coal breaking process, properties, and mechanisms.

The moisture, an existing component in coal and air, can be adsorbed on the coal pores surface by connecting with the oxygen-containing functional groups or hydrogen bonds [18]. Besides, the precipitation of moisture in coal can cause the collapse of large and medium pores, thereby shrinking its volume. The raw pore structure could change because the gel structure in coal collapses when the moisture escapes during drying process [19]. It means that the moisture content in raw coal is not only related with microstructure characteristics, but also its absorption or desorption during coal transmission and storage before crushing can significantly affect the microstructures. Incorporating with the previous studies: Zhang et al. found that the indentation modulus of coal decreased after water absorption, and they attributed it to change of microstructure led by water adsorption [11]. Besides, Xin et al. discovered that drying coal easily leaded to changes of pore structure [12]. Thus, it can be reasonably speculated that the moisture in raw coal can also affect the microstructures and then cause changes of its mechanical and crushing properties [20]. Therefore, it is of great significance to deeply study the influence of moisture on coal mechanical properties during crushing process.

In addition, industrial coal crushing process is not an instantaneous process and the coal is actually broken by the cyclic action of external force. Under cyclic loading process, the breaking of coal is accompanied by energy dissipation, which increases steadily with the load level rising [21]. Meanwhile, as the cyclic loading times increases, the destruction of the coal microstructures becomes more severe, and the channel is formed between the pores [22, 23]. So it is of great significance to study the cumulative crushing effect of coal under cyclic loading based on evolution characteristics of microstructures. Besides, from the experiments about the effects of cyclic loading on rocks, the failure mode of the rocks under cyclic loading is very different from the failure mode under static loading. More local cracks are observed under cyclic loading process [24], and cyclic loading can cause rock cracks at lower loads [25]. Based on the micro-crack density, it is found that the damage of coal microstructures continues to increase with progress of the cycle, which results in some changes in the spatially related length [26]. In addition, in the cyclic loading experiment of artificial jointed rock, it is found that with increase of the maximum stress, the damage after circulation becomes greater and develops faster [27]. Obviously, the loading method and stress also have a significant effect on the rock crushing characteristics [24, 27]. Besides, as for coal, it can be speculated that the cyclic loading can also have significant but different effects on the mechanical properties as static loading. Further exploring the microstructures and mechanical properties of coal under cyclic loading is key to understand cumulative crushing effects.

In this work, three typical Chinese bituminous coals were chosen, the effects of moisture content and cyclic loading during coals crushing process were investigated. The images of coals surfaces and mechanical properties were recorded with a high-speed camera and a microcomputer-controlled electronic universal testing machine respectively. The roles of moisture content and cyclic loading in microstructures and their effects on mechanical properties were revealed. The evolution process of coal microstructures was quantified with the fractal dimension, and a universal relationship between microstructures and mechanical properties was finally established.

2. Experimental and methods

2.1 Experimental materials and process

Three bituminous Chinese coals (SM, HSQ, and WCW) were from Shenmu coal mine in Shaanxi province, Hongshaquan coal mine and Wucaiwan coal mine in Xinjiang province respectively. Proximate and ultimate analysis of the three raw coals are shown in our previous work [13]. Before experiments, the raw coals were uniformly cut and polished to small cube lumps (1.0 cm × 1.0 cm × 1.0 cm). Firstly, the lump coals were fully immersed in deionized water for 12 hours to achieve water-saturated, and then the water-saturated samples were placed in an oven at 120 ℃ for drying until their weights no longer decreased. In this condition, the moisture can be evaporated, and it can guarantee that its chemical structures were not destroyed [28]. Because these three coals possessed different initial moisture contents and distinct abilities to adsorb moisture, leading to the phenomenon that their moisture contents are varied at water-saturated situation. In order to compare them more accurately, the relative moisture content (RMC, %) during coal drying process was defined according to Eq. (1).

$$RMC = \frac{M - M_\infty}{M_0 - M_\infty} \times 100\% \tag{1}$$

Where M_0 (g) meant the mass of the saturated sample, M_∞ (g) was the mass of dried samples, and M (g) represented the mass of these samples at any time during drying process.

The change of relative moisture content in three coals with drying time was recorded and shown in Fig. S1. Different relative moisture contents (100%, 75%, 50%, 25%, and 0%) were selected and their corresponding drying times are shown in Table 1. Fig. 1 shows the diagram of experimental devices, and all the uniaxial load experiments were done on the microcomputer-controlled electronic universal testing machine. During the experiment, the lump coal was placed on the universal base, and then it was loaded by uniaxial load at a speed of 5 mm/min. At the same time, the microstructures on coal surface were recorded on-line with a high-speed camera at a frequency of 50 frames/second. Subsequently, SM (the raw coal) was further selected to conduct the cyclic loading experiments, because the compressive strength of SM was much larger than HSQ and WCW, suggesting SM needed more times to achieve crush, indicating that SM can be more appropriate to study the effects of cyclic loading. In order to improve the accuracy of the results, the average compressive strength for 100% stress level was measured based on five samples by uniaxial load mechanical experiments, and the results are shown in Fig. S2, from which the average compressive strength was calculated to be 16.71 MPa for 100% stress level. The other stress levels (60%, 70%, 80%, and 90%) were calculated based on 100% stress level, and they were 10.03 MPa, 11.70 MPa, 13.37 MPa, and 15.04 MPa respectively. The loading forces in constant stress and variable stress cyclic loading experiments were calculated by multiplying the cross-sectional area.

2.2 Analysis methods

In order to reflect the mechanical properties of coals uniformly, the force and displacement were recorded, and the stress (σ, MPa) and strain (ε) during uniaxial load experiments were calculated according to the following equations:

$$\sigma = \frac{F}{S_0} \tag{2}$$

$$\varepsilon = \frac{\Delta L}{L_0} \tag{3}$$

where F (N) was the force during uniaxial load, S_0 (m^2) meant the cross-sectional area, ΔL (mm) was the deformation during experiment, and L_0 (mm) represented the original height.

From the images of coal surface during uniaxial load experiments, it can be observed that the cracks develop and lump coal breaks irregularly, which are typical fractal characteristics [29]. In order to eliminate the differences between initial structures of coals, the relative stress (σ_r, MPa) and relative fractal dimension (D_r) were defined to characterize the mechanical properties and microstructures based on our previous work [13]:

$$\sigma_r = \frac{\sigma}{\sigma_{max}} \tag{4}$$

$$D_r = \frac{D - D_{min}}{D_{max} - D_{min}} \tag{5}$$

Where σ_{max} (MPa) was the maximum stress value in the experiment, σ (MPa) meant the stress value at any time, D_{max} and D_{min} were the maximum and minimum fractal dimensions, and D was the fractal dimension.

In order to better describe the cumulative process of coal crushing during cyclic loading, the strain variable was selected to quantitate the degree of crushing damage. The new strain in n-th cycle was assumed as ε_n, and in fact, the strain after n-th cycle in the stress-strain curve was the cumulative strain of n times as ε_N in Eq. (6).

$$\varepsilon_N = \Sigma(\varepsilon_n) \tag{6}$$

3. Results and discussion

3.1 Typical coal crushing process under the uniaxial load experiment

Taking raw SM for example, a typical stress-strain curve and corresponding images of the coal surface during uniaxial load experiment are shown in Fig. 2. Four stages that are compaction stage (stage A), elastic deformation stage (stage B), plasticity deformation stage (stage C), and fracture residual stage (stage D) are clearly observed respectively. From the images, it can be seen that the lump coal gradually deforms under uniaxial compression load, and new crack occurs and extends until it is broken. In stage A, the stress increases slowly, and no obvious cracks on coal surface are observed, indicating the microstructure is intact in this stage. In stage B, the stress increases continuously and the stress-strain curve is approximately a straight line, where the slope of the stress-strain curve is elastic modulus. In this stage, few cracks can be observed on the coal surface as the stress does not pass breaking limit and the structure remains unbroken. In stage C, the stress reaches and passes through the highest point (compressive strength), and obvious cracks appear on the coal surface, suggesting the lump coal microstructures suffer severe damages. Besides, the extension of the cracks leads to a rapidly drop of supporting capacity. In stage D, the stress drops sharply, new cracks continue to appear on the coal surface, and then gradually fill wholly. At this time, the lump coal is completely broken, and its initial appearance is lost.

3.2 Effects of moisture on the microstructures and mechanical properties

3.2.1 Effects of moisture on the microstructures

The relative fractal dimensions at different moisture contents during drying process of three coals are drawn in Fig. 3. As seen clearly, with the decrease of relative moisture content, the relative fractal dimension of SM does not take on an evident tendency, while the relative fractal dimensions of HSQ and WCW gradually increase. It indicates that drying process cannot significantly damage the microstructures of SM, but the cracks on HSQ and WCW surfaces gradually develop. This is because that the moisture desorption process can significantly affect the microstructures of HSQ and WCW, which improves the internal pore diameter during drying process, resulting in the production of internal force and cracks on coal surface [30]. Besides, it can be seen that the relative fractal dimensions of HSQ and WCW change rapidly when the relative moisture content decreases from 75% to 25%, revealing that the microstructures are severely damaged at this stage. The relative moisture content between 75% and 25% is a key range that should be paid attention to during the coal crushing process.

3.2.2 Effects of moisture on mechanical properties

Fig. 4 shows the relationship between compressive strength and elastic modulus for coals with different relative moisture contents. It can be seen that there is a strong positive linear relationship between the compressive strength and elastic modulus for these three coals with different relative moisture contents, whose fitted equation is as Eq. (7) and the R^2 can be as high as 0.94. Thus, this equation is suitable for these three coals with various relative moisture contents. With assists of this equation, the compressive strength can be predicted by elastic modulus that can be calculated in the initial stage B (in Fig. 2). It means the compressive strength can be predicted on the premise of keeping the lump coal unbroken, which provides a new way for efficient and quick measurement of the compressive strength of coal with different relative moisture contents.

$$Y = 42.69X + 71.18 \tag{7}$$

The compressive strengths and elastic modules of coals at different relative moisture contents are shown in Fig. 5, from which it can be seen that the change trends of the compressive strength and elastic modulus for the same coals are similar with the change of relative moisture content. The change trend is also consistent with the linear relationship between compressive strength and elastic modulus.

However, the values of compressive strengths and elastic modulus of different coals are various, and the tendencies of them with relative moisture content decreasing take on two types: (1) The compressive strength and elastic modulus of HSQ and WCW decreases as the relative moisture content decreases, and they are lowered to a minimum value when the relative moisture content is about 25%, and then increase slightly; (2) The compressive strength and elastic modulus of SM show an inverse change tendency with HSQ and WCW, they gradually increase with relative moisture content decreasing. This is because that moisture in the coals mainly possesses two effects on mechanical properties, which are strongly related with the coal porosity [30-33]: (1) High coal porosity can assist in adsorbing more moistures. Moisture desorption would cause obvious internal pore diameter improvement, thus resulting in internal force and cracks on the coal structures. In this situation, lower moisture content can lead to the phenomenon that coal is easier to be broken; (2) Low coal porosity can assist in adsorbing less moistures. Moisture adsorption would mainly play roles in softening and lubricating coal. In this situation, higher moisture content can lead to the phenomenon that coal is easier to be broken. Our previous study has shown that the porosities of HSQ, WCW and SM are 22.8%, 29.7%, and 10.8% respectively [13]. As a result of the rich porosity, the mass ratios of moisture for HSQ and WCW at saturated state are 33.05% and 38.54% respectively. While the mass ratio of moisture for SM is only 7.10% at saturated state. The evaporation of moisture could cause obvious damages on the microstructures during the drying process for HSQ and WCW, which is also consistent with the results of Fig. 3. As for SM, the drying process possesses little damage effects on the microstructures, thus the softening and lubricating effects are key to weak mechanical properties when the relative moisture content is high. Therefore, when the relative moisture content of SM is 100%, the lump coal is most easily broken. And as the relative moisture content reduces, both the softening effect and lubricating effect from moisture on the internal bedding of the coal decrease, resulting in a rise of the compressive strength and elastic modulus of the lump coal. While when the relative moisture contents of HSQ and WCW are higher, the lump coals are almost more difficult to be broken. In summary, as for coals with different porosities, the moisture of coals possesses distinct effects on their mechanical properties, which should be valued during the coal crushing process.

3.3 Effects of cyclic loading on microstructures and mechanical properties

3.3.1 Effects of cyclic loading on microstructures

As for SM (the raw coal), the changes of relative fractal dimension with cyclic loading times increasing under constant and variable stresses cyclic loading are exhibited in Fig. 6. As a whole, under the initial cycles, the surface does not change, but the internal structures are damaged gradually, which causes the further change of the surface microstructures under the next action. As the number of cycles reaches a certain amount, the internal structures changes accumulated to a critical point, and the microstructures evolve rapidly. However, the detailed break processes and characteristics under constant and variable stresses are different.

Taking 70% stress level for example (Fig. 6 (a)), it can be found that the change of the relative fractal dimension can be divided into four stages during the constant cyclic loading process. Firstly, the relative fractal dimension remains basically unchanged in the first four cyclic loads, following which the relative fractal dimension increases significantly under the 5th load. Then the relative fractal dimension at 6-8th cyclic loads does not change significantly. The relative fractal dimensions both increase significantly after 9th and 10th loads, and the coal structures are destroyed. It indicates that the microstructures become more complicated as damage degree deepens. During this process, new cracks continuously generate and gradually penetrate, and they change greatly in the later stage of cyclic loading. After the last cyclic load, the work effects by external force change from quantitative to qualitative. The coal structures are destroyed, and the lump coal is thus broken.

During the variable stress cyclic loading experiments, the relative fractal dimension also changes with the increase of cyclic times (Fig. 6 (b)), revealing that the coal microstructures change obviously with the increase of cyclic times. At 60% and 70% stress levels, when the cyclic times increases, the relative fractal dimension only changes slightly, indicating that the load mainly produces elastic deformation at this process, and the microstructures have not been destroyed. When the stress level increases to 80%, the relative fractal dimension increases significantly from 0.05 to 0.71, suggesting that 80% stress level can produce obvious effects on the increase of its fractal dimension [34]. At this stage, the lump coal has obvious plastic deformation, and the changes of coal microstructures are significantly obvious. Then the microstructures continue to change under 90% stress load until the lump coal is finally broken.

3.3.2 Effects of cyclic loading on mechanical properties

In order to explore the corresponding changes in mechanical characteristics of lump coals during cyclic loading process, taking 70% stress level for example, the stress-strain curve is shown in Fig. S3. It can be clearly seen that during the constant stress cyclic loading, a stress-strain hysteresis curve generates in each cycle. Besides, with increase of cycles, new strains gradually generate, and the stress-strain hysteresis curve gradually shifts to the right. After the last cyclic load, the lump coal is broken. The cumulative work has reached the energy required for coal break, indicating that the coal crushing process is gradually cumulative. Besides, the strain accumulation and cyclic load times under constant stress of SM at 70% stress level are shown in Fig. S4. It shows that during the cyclic loading process, the cumulative amount of strain gradually increases as the number of cycles continuously increases, which indicates that the effect of loading on coal gradually deepens. When the lump coal is broken, the strain accumulation reaches the maximum value. Meanwhile, the changes of microstructures for SM are obvious after the 5th, 9th, and 10th cycles, it is consistent with the results in Fig. 6 (a) that the strain accumulation of SM also increases more significantly after 5th, 9th, and 10th cycles, which also proves that greater increase in strain would lead to more obvious changes of the microstructures in the coal surface.

In the process of variable stresses cyclic loading (from 60% stress level to 100% stress level) for the raw SM coal, the strain accumulation can quantitatively describe the crushing degree, and the results are shown in Fig. 7. During the cyclic loading of the same stress levels, the strain accumulation increases slowly with the increase of cycle times. However, when the cyclic load stress level increases, the strain accumulation would increase significantly. The cumulative effect of strain shows a step-up state, which indicates that the increased force process possesses a significant effect on the coal destruction.

Fig. 8 shows the average proportion of strain generated by 25 cycles of SM1-SM4. It can be seen that first cyclic load can produce the largest strain proportion (72.05%). In addition, the load of first cyclic time after increase of stress level is also significantly greater than those of 2-5 cyclic times. Except for the first load of each stress level (1st, 6th, 11th, 16th, and 21th times), the remaining 20 loads account for a small proportion of the strain with an average proportion of 0.36%. These results directly show that the effect of cyclic loading under constant force on coal is far less than the effect of gradual increased force, suggesting that the coal crushing process with a gradual increased stress level is preferred.

3.4 Relationship between microstructures and mechanical properties

Previous researches have shown that mechanical properties are strongly related with the microstructures of coals during crushing process [35, 36]. However, no universal relationship has been built yet. Thus, in order to build the universal relationship between coal microstructures and mechanical properties during coal crushing process, the experimental data of the relative fractal dimensions and relative stresses are fitted in Fig. 9, and quantitative relationship can be expressed as Eq. (8), for which the R^2 can be as high as 0.85.

$$\sigma_r = -0.67D_r^2 + 1.62D_r + 0.07 \tag{8}$$

As a whole, it can be obviously seen that as the relative fractal dimension increases, the relative stress shows an upward trend, and the trend is universally applicable for the three coals with various relative moisture contents. So the mechanical properties can be acquired by the relative fractal dimensions of coal surface images, and the relative error is expected to be very small. Besides, in the variable stresses cyclic loading experiments of SM, the relative fractal dimension with the change of relative stress can also fit to the relationship interestingly. Furthermore, the quantitative relationship excludes the effect of these three Chinese bituminous coals under different moisture contents and cyclic loading through two dimensionless parameters of relative fractal dimension and relative stress, and only focuses on the relationship between the microstructures and mechanical properties during coal crushing process. It reveals that the association between microstructures and mechanical properties, indicating that mechanical properties of coal could be predicted by its surface images, which is extremely important and significant to guide coal grinding crushing.

4. Conclusions

Taking typical Chinese bituminous coals as research objectives, the roles of moisture and cyclic loading in microstructures and their effects on mechanical properties were detailedly investigated, and main conclusions can be drawn as follows:

(1) The effects of moisture on the mechanical properties for the coals strongly depended on porosity. For low porosity coal (SM), moisture mainly softened and lubricated, thus reducing the compressive strength and elastic modulus. For high porosity coal (HSQ and WCW), moisture desorption process would create some cracks and fractures, thus reducing compressive strength and elastic modulus.

(2) Under the cyclic loading process, the cumulative effect of strain showed a step-up state under different stress levels. The first load in the cyclic loading produced the largest strain, and caused the most obvious damage on coal structures.

(3) The mechanical properties of raw coals were strongly related with their microstructures. There was a normalized quantitative relationship between the relative stress and relative fractal dimension during coal crushing, which can be expressed as $\sigma_r = -0.67D_r^2 + 1.62D_r + 0.07$.

Acknowledge

This work was financially supported by the National Natural Science Foundation of China (No. 51576072, No. 51806073, No. 21908156, U1910214). The authors also acknowledge the extended help from Analytical and Testing Center of Huazhong University of Science and Technology.

References

[1] BP Energy Outlook, 2019. https://www.bp.com/en/global/corporate/energy-economics/energy-outlook.html.

[2] Xu J., Tang H., Su S., Liu J., Xu K., Qian K., et al. A study of the relationships between coal structures and combustion characteristics: The insights from micro-Raman spectroscopy based on 32 kinds of Chinese coals. Applied Energy 2018; 212: 46-56. https://doi.org/10.1016/j.apenergy.2017.11.094.

[3] Zhou W., Wang H., Wang D., Zhang K., Du Y., Yang H.. The effect of geometries and cutting parameters of conical pick on the characteristics of dust generation: Experimental investigation and theoretical exploration. Fuel Processing Technology 2020; 198: 106243. https://doi.org/10.1016/j.fuproc.2019.106243.

[4] He Y., Xie W., Zhao Y., Li H., Wang S.. Triboelectrostatic separation of pulverized fuel of coal power plant based on mineralogical analyses. International Journal of Mineral Processing 2017; 166: 7-12. https://doi.org/10.1016/j.minpro.2017.06.005.

[5] Xie W., He Y., Yang Y., Shi F., Huang Y., Li H., et al. Experimental investigation of breakage and energy consumption characteristics of mixtures of different components in vertical spindle pulverizer. Fuel 2017; 190: 208-220. https://doi.org/10.1016/j.fuel.2016.11.026.

[6] Sung Y., Moon C., Eom S., Choi G., Kim D.. Coal-particle size effects on NO reduction and burnout characteristics with air-staged combustion in a pulverized coal-fired furnace. Fuel 2016; 182: 558-567. https://doi.org/10.1016/j.fuel.2016.05.122.

[7] Pan R., Qiu T., Chao J., Ma H., Wang J., Li C.. Thermal evolution of the oxidation

characteristics of pulverized coal with different particle sizes and heating rates. Thermochimica Acta 2020; 685: 178516. https://doi.org/10.1016/j.tca.2020.178516.

[8] Liu X., Tan Y., Ning J., Lu Y., Gu Q.. Mechanical properties and damage constitutive model of coal in coal-rock combined body. International Journal of Rock Mechanics and Mining Sciences 2018; 110: 140-150. https://doi.org/10.1016/j.ijrmms.2018.07.020.

[9] Dong J., Cheng Y., Hu B., Hao C., Tu Q., Liu Z.. Experimental study of the mechanical properties of intact and tectonic coal via compression of a single particle. Powder Technology 2018; 325: 412-419. https://doi.org/10.1016/j.powtec.2017.11.029.

[10] Chen S., Yin D., Jiang N., Wang F., Zhao Z.. Mechanical properties of oil shale-coal composite samples. International Journal of Rock Mechanics and Mining Sciences 2019; 123: 104120. https://doi.org/10.1016/j.ijrmms.2019.104120.

[11] Zhang Y., Lebedev M., Al-Yaseri A., Yu H., Xu X., Sarmadivaleh M., et al. Nanoscale rock mechanical property changes in heterogeneous coal after water adsorption. Fuel 2018; 218: 23-32. https://doi.org/10.1016/j.fuel.2018.01.006.

[12] Xin F., Xu H., Tang D., Cao L.. An improved method to determine accurate porosity of low-rank coals by nuclear magnetic resonance. Fuel Processing Technology 2020; 205: 106435. https://doi.org/10.1016/j.fuproc.2020.106435.

[13] Shan L., Hu S., Zhang Y., Wu P., Xu K., Xu J., et al. Relationship between fractal meso-structural and mechanical characteristics of lump coal under uniaxial compression at different temperatures. Fuel Processing Technology 2019; 194: 106112. https://doi.org/10.1016/j.fuproc.2019.05.035.

[14] Yu H., Zhang Y., Lebedev M., Han T., Verrall M., Wang Z., et al. Nanoscale

geomechanical properties of Western Australian coal. Journal of Petroleum Science and Engineering 2018; 162: 736-746. https://doi.org/10.1016/j.petrol.2017.11.001.

[15] Xu J., Liu J., Zhang X., Ling P., Xu K., He L., et al. Chemical imaging of coal in micro-scale with Raman mapping technology. Fuel 2020; 264: 116826. https://doi.org/10.1016/j.fuel.2019.116826.

[16] Li Y., Yang J., Pan Z., Tong W.. Nanoscale pore structure and mechanical property analysis of coal: An insight combining AFM and SEM images. Fuel 2020; 260: 116352. https://doi.org/10.1016/j.fuel.2019.116352.

[17] Hu S., Shan L., Xu B., Su J., Wang Y., Jiang L., et al. Meso-mechanical properties evolution during fracture of coal cubes under loading. Journal of China Coal Society 2018; 43: 855-861. https://doi.org/10.13225/j.cnki.jccs.2017.0970.

[18] Charrière D., Behra P.. Water sorption on coals. Journal of Colloid and Interface Science. 2010; 344: 460-467. https://doi.org/10.1016/j.jcis.2009.11.064.

[19] Yu J., Tahmasebi A., Han Y., Yin F., Li X.. A review on water in low rank coals: The existence, interaction with coal structure and effects on coal utilization. Fuel Processing Technology 2013; 106: 9-20. https://doi.org/10.1016/j.fuproc.2012.09.051.

[20] Zhang Q., Fan X., Chen P., Ma T., Zeng F.. Geomechanical behaviors of shale after water absorption considering the combined effect of anisotropy and hydration. Engineering Geology 2020; 269: 105547. https://doi.org/10.1016/j.enggeo.2020.105547.

[21] Song D., Wang E., Liu J.. Relationship between EMR and dissipated energy of coal rock mass during cyclic loading process. Safety Science 2012; 50: 751-760. https://doi.org/10.1016/j.ssci.2011.08.039.

[22] Jiang C., Duan M., Yin G., Wang J., Lu T., Xu J., et al. Experimental study on seepage properties, AE characteristics and energy dissipation of coal under tiered cyclic loading. Engineering Geology 2017; 221: 114-123. https://doi.org/10.1016/j.enggeo.2017.03.005.

[23] Pan R., Ma Z., Yu M., Chao J., Li C., Wang J.. Study on the mechanism of coal oxidation under stress disturbance. Fuel 2020; 275: 117901. https://doi.org/10.1016/j.fuel.2020.117901.

[24] Geranmayeh Vaneghi R., Ferdosi B., Okoth A., Kuek B.. Strength degradation of sandstone and granodiorite under uniaxial cyclic loading. Journal of Rock Mechanics and Geotechnical Engineering 2018; 10: 117-126. https://doi.org/10.1016/j.jrmge.2017.09.005.

[25] Erarslan N.. Microstructural investigation of subcritical crack propagation and Fracture Process Zone (FPZ) by the reduction of rock fracture toughness under cyclic loading. Engineering Geology 2016; 208: 181-190. https://doi.org/10.1016/j.enggeo.2016.04.035.

[26] Zhang Z., Wang E., Li N., Li X., Wang X., Li Z.. Damage evolution analysis of coal samples under cyclic loading based on single-link cluster method. Journal of Applied Geophysics 2018; 152: 56-64. https://doi.org/10.1016/j.jappgeo.2018.03.014.

[27] Liu M., Liu E.. Dynamic mechanical properties of artificial jointed rock samples subjected to cyclic triaxial loading. International Journal of Rock Mechanics and Mining Sciences 2017; 98: 54-66. https://doi.org/10.1016/j.ijrmms.2017.07.005.

[28] Feng L., Yuan C., Mao L., Yan C., Jiang X., Liu J., et al. Water occurrence in lignite and its interaction with coal structure. Fuel 2018; 219: 288-295. https://doi.org/10.1016/j.fuel.2018.01.097.

[29] Zhou S., Liu D., Cai Y., Yao Y.. Fractal characterization of pore-fracture in low-rank coals

using a low-field NMR relaxation method. Fuel 2016; 181: 218-226. https://doi.org/10.1016/j.fuel.2016.04.119.

[30] Yang X., Jiang Y., Shao X.. Drying intensity affected to pore structure and water re-adsorption in lignite. Coal Science and Technology 2014; 42: 109-112. https://doi.org/10.13199/j.cnki.cst.2014.04.028.

[31] Sampath K., Perera M., Li D., Ranjith P., Matthai S.. Evaluation of the mechanical behaviour of brine+CO_2 saturated brown coal under mono-cyclic uni-axial compression. Engineering Geology 2019; 263: 105312. https://doi.org/10.1016/j.enggeo.2019.105312.

[32] Zhang X., Ranjith P., Lu Y., Ranathunga A.. Experimental investigation of the influence of CO2 and water adsorption on mechanics of coal under confining pressure. International Journal of Coal Geology 2019; 209: 117-129. https://doi.org/10.1016/j.coal.2019.04.004.

[33] Zhong C., Zhang Z., Ranjith P., Lu Y., Choi X.. The role of pore water plays in coal under uniaxial cyclic loading. Engineering Geology 2019; 257: 105125. https://doi.org/10.1016/j.enggeo.2019.05.002.

[34] Yu B., Chen Z., Wu J.. Experimental study on compaction and fractal characteristics of saturated broken rocks with different initial gradations. Journal of Mining & Safety Engineering 2016; 33: 342-347. https://doi.org/10.13545/j.cnki.jmse.2016.02.024.

[35] Hu S., Su J., Xu B., Shan L.. Surface structure evolution of coal cubes during compression process and its relationship with mechanical properties. Huazhong Univ. of Sci & Tech. (Natural Science Edition) 2017; 45: 118-122. https://doi.org/10.13245/j.hust.170122.

[36] Xu H., Wang G., Fan C., Liu X., Wu M.. Grain-scale reconstruction and simulation of coal mechanical deformation and failure behaviors using combined SEM Digital Rock data and

DEM simulator. Powder Technology. 2020; 360: 1305-1320. https://doi.org/10.1016/j.powtec.2019.07.014.

Tables

Table 1 Drying time of relative moisture content for the three coals (min)

RMC	100%	75%	50%	25%	0%
SM	0	34	80	150	300
HSQ	0	17	52	110	300
WCW	0	13	43	95	300

459 # Figures

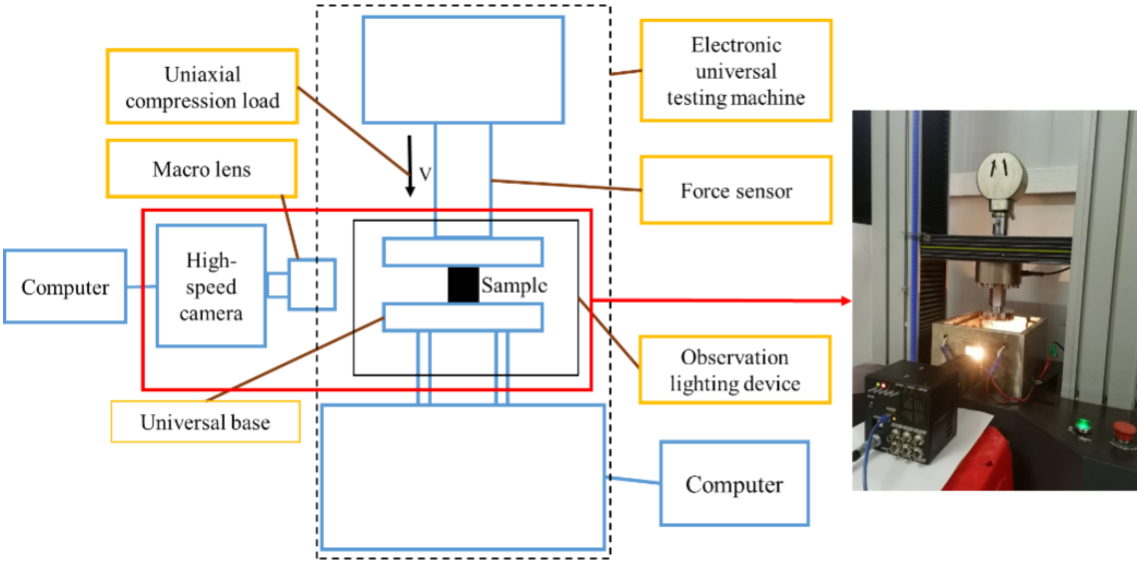

Fig. 1. Diagram of experimental devices

460

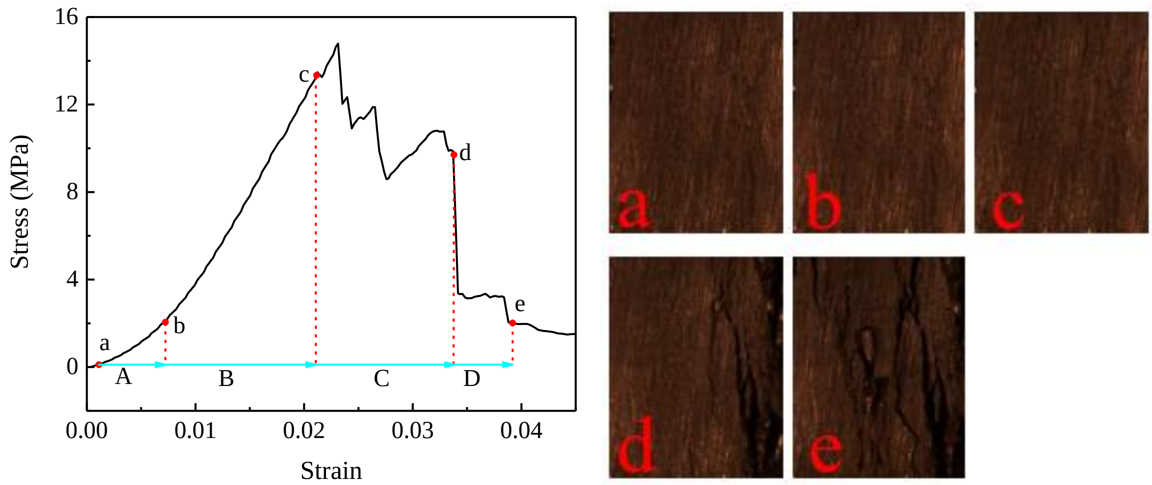

Fig. 2. Typical stress points and corresponding coal surface images for SM

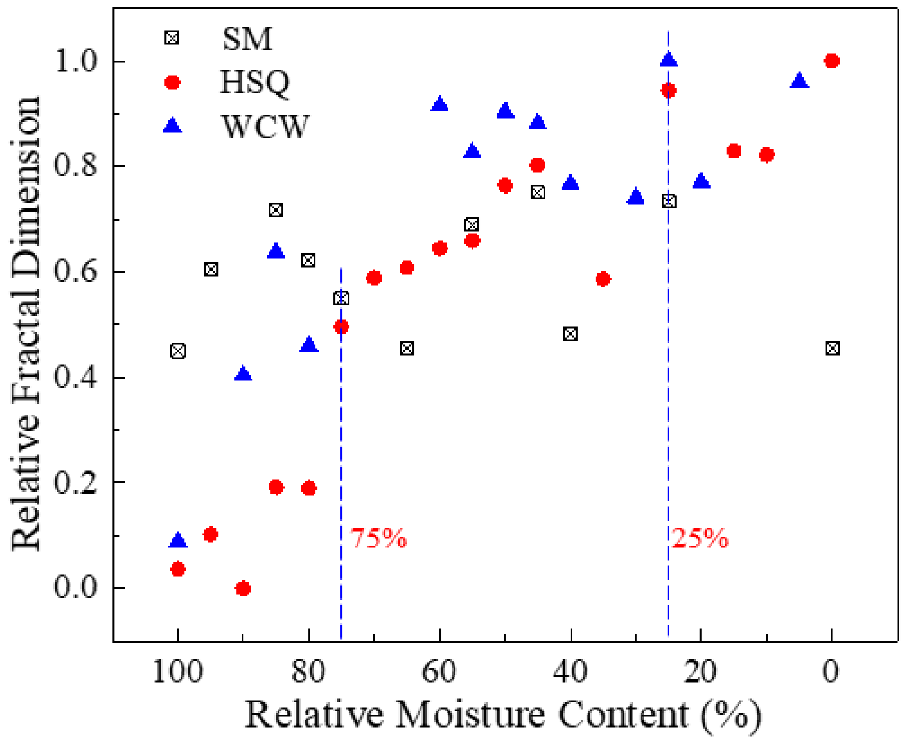

Fig. 3. The relative fractal dimension at different moisture contents during drying process of three coals

462

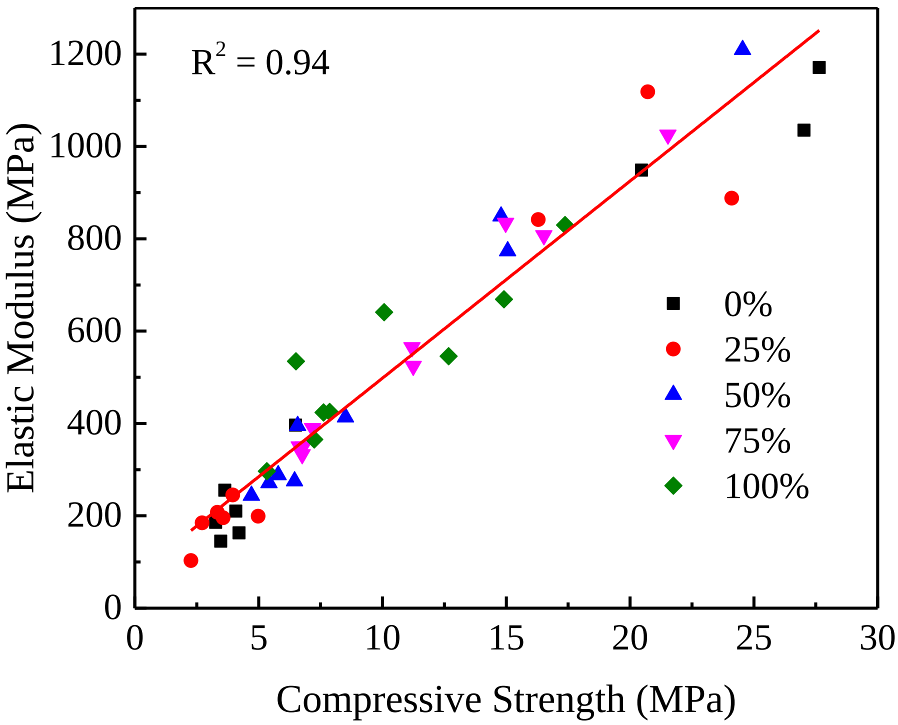

Fig. 4. Relationship between compressive strength and elastic modulus for coals with different relative moisture contents

463

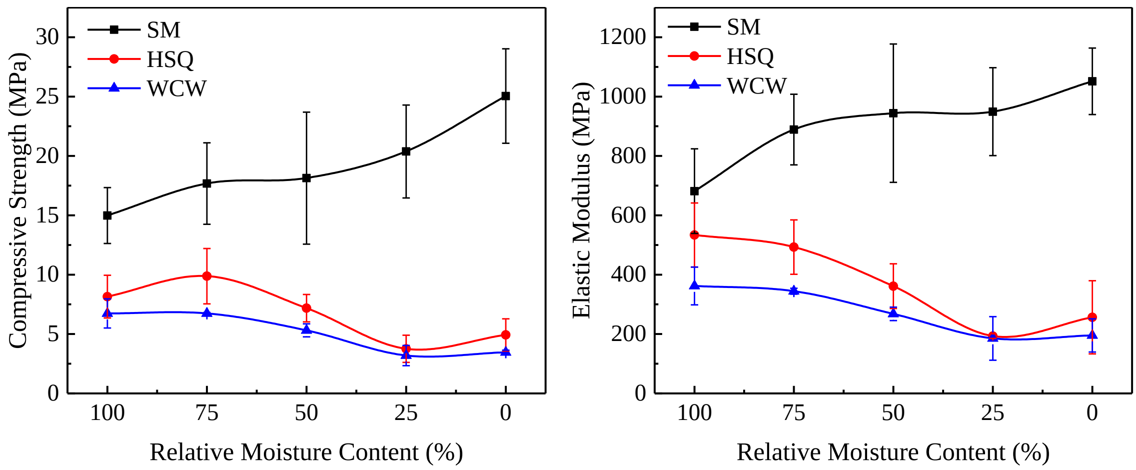

Fig. 5. Compressive strength and elastic modulus of three coals with different moisture contents

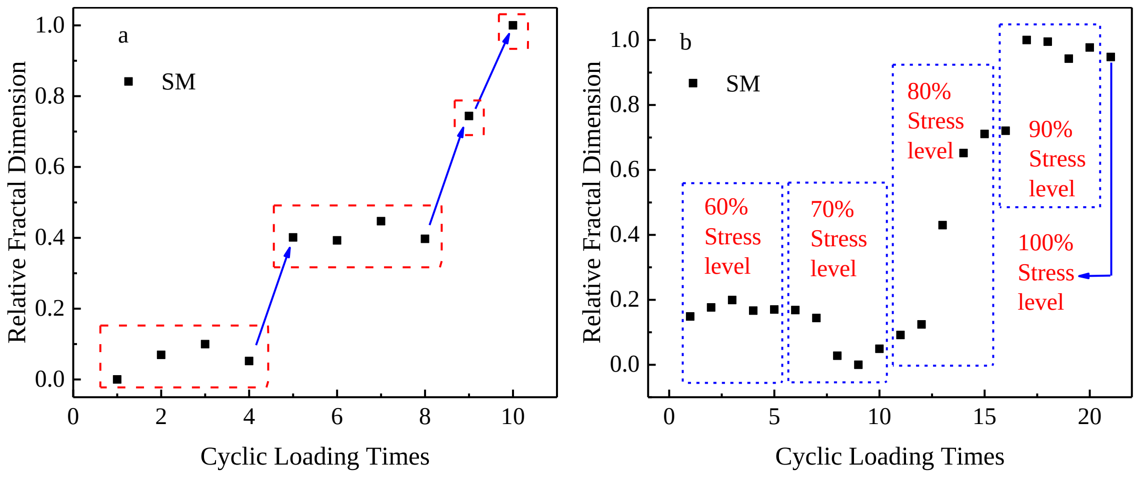

Fig. 6. Microstructures evolution of SM: (a) Under constant stress cyclic loading (70% stress level), (b) Under variable stress cyclic loading

465

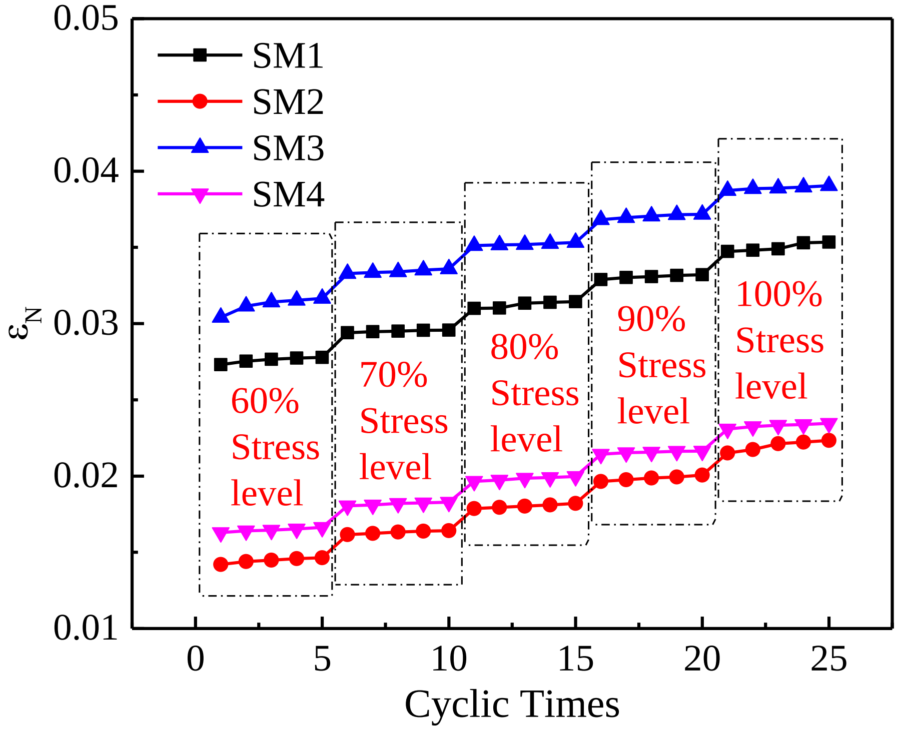

Fig. 7. Strain accumulation under cyclic loading with variable stress

466

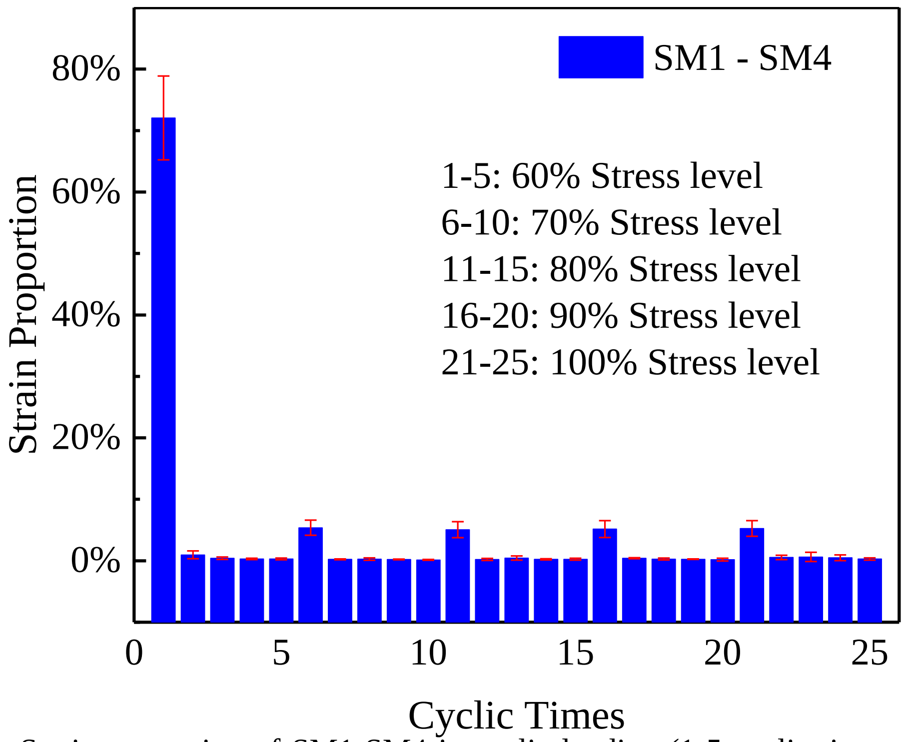

Fig. 8. Strain proportion of SM1-SM4 in cyclic loading (1-5 cyclic times: 60% stress level, 6-10 cyclic times: 70% stress level, 11-15 cyclic times: 80% stress level, 16-20 cyclic times: 90% stress level, 21-25 cyclic times: 100% stress level)

467

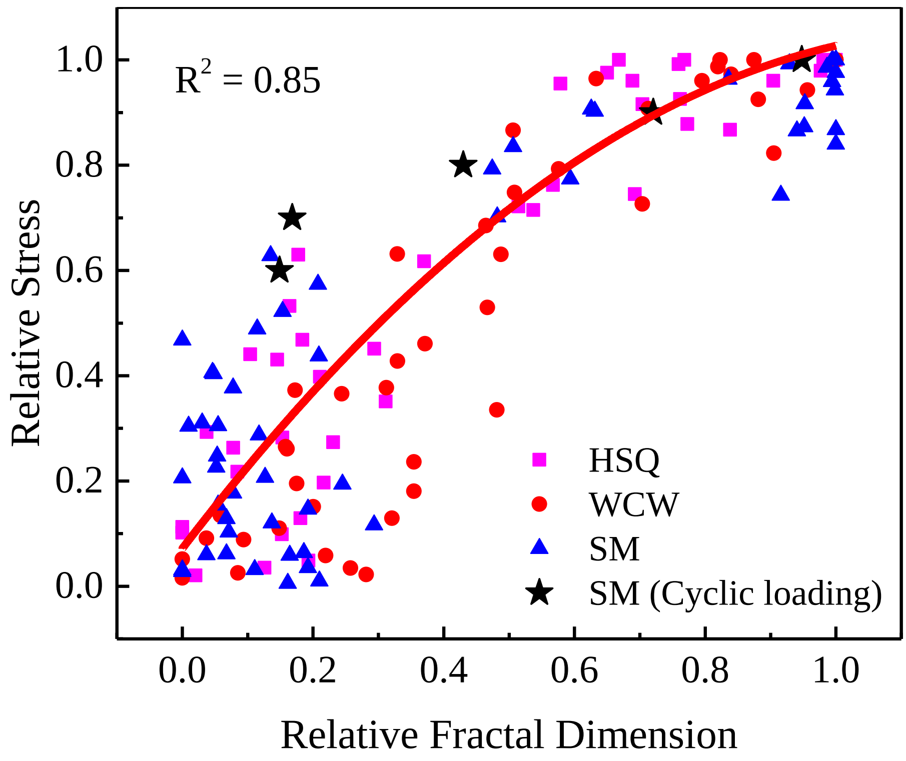

Fig. 9. Relationship between relative fractal dimension and relative stress of three coals

468

TITLE PAGE

- **TITLE**

Roles of moisture and cyclic loading in microstructures and their effects on mechanical properties for typical Chinese bituminous coals

- **Authors and affiliations**

Qiangqiang Ren [a], Yufei Zhang [a, c], Inmaculada Arauzo [b, c], Lianying Shan [a, c], Jun Xu [a, *], Yi Wang [a, c], Sheng Su [a, c], Song Hu [a, c, *], Jun Xiang [a, c]

[a] State Key Laboratory of Coal Combustion, School of Energy and Power Engineering, Huazhong University of Science and Technology, Wuhan 430074, China

[b] Department of Mechanical Engineering, University of Zaragoza, Mariano Esquillor 15, E-50018 Zaragoza, Spain

[c] China-EU Institute for Clean and Renewable Energy, Huazhong University of Science and Technology, Wuhan 430074, China

- **Corresponding authors**

State Key Laboratory of Coal Combustion, School of Energy and Power Engineering, Huazhong University of Science and Technology, Wuhan 430074, China

Tel.: +86-27-87542417, Fax: +86-27-87545526

E-mail: xujun_sklcc@hust.edu.cn (Jun Xu), husong_hust@hotmail.com (Song Hu).

Abstract:

This work aimed at studying the roles of moisture and cyclic loading in microstructures and their effects on mechanical properties for typical Chinese bituminous coals. Different relative moisture contents (100%, 75%, 50%, 25%, and 0%) for Shenmu coal (SM), Hongshaquan coal (HSQ), and Wucaiwan coal (WCW) were chosen to study the effects of moisture. The raw SM was then further selected to investigate the effects of cyclic loading. Images of coals surfaces and mechanical properties during simulated crushing process were recorded and combined to be analyzed. The results showed that the moisture possessed significant effects on coal mechanical properties, which strongly depended on their porosities. As for low porosity coal (SM), the adsorption of moisture can soften and lubricate the microstructures, weakening mechanical properties. While the drying process would destroy the microstructures and decease mechanical properties for high porosity coals (HSQ and WCW). Under the cyclic loading process, the cumulative effects of strain showed a step-up state and the first cyclic loading can typically cause biggest change of microstructures and produce the largest strain under different stress levels. Finally, a normalized quantitative relationship ($\sigma_r = -0.67D_r^2 + 1.62D_r + 0.07$) between the relative fractal dimension and relative stress was built.

Keywords: bituminous coal; moisture; cyclic loading; crushing; microstructures; mechanical properties.

1. Introduction

Coal, a key fuel, will still occupy 20% energy consumption in the world, and even over 50% in many developing countries such as China, India, South Africa, and so on as estimated by 2040 [1-3]. As it is widely known that the utilization of coal cannot be separable from the crushing process, by which higher coal conversion efficiency and lower pollutant emissions can be achieved [4]. But, the coal crushing process would consume huge quantities of energy, even about 1% of the electricity produced by coal-fired power plant [5]. Besides, coal crushing process is also an extremely complex process [6, 7]. Deeply studying the properties and mechanisms of coal crushing process is key for saving energy and efficient coal utilization.

The essence of coal crushing process is the deformation of physical structure [8, 9] and the crushing process is closely related to the mechanical properties of raw coal [8, 10]. Besides, it has been directly shown by the previous researches that the mechanical properties of coal were not only affected by the external environment such as moisture [11-12] and heating [13], but also by the internal factors such as composition [2, 14, 15] and pore structure [16, 17]. These factors either cause the change of microstructures or thus affect the mechanical properties of coal. However, the effects of some typical external factors on internal microstructures have not been fully studied yet, while the relationship between the coal microstructures and mechanical properties has not been quantitatively understood, which can assist to further reveal the coal breaking process, properties, and mechanisms.

The moisture, an existing component in coal and air, can be adsorbed on the coal pores surface by connecting with the oxygen-containing functional groups or hydrogen bonds [18]. Besides, the precipitation of moisture in coal can cause the collapse of large and medium pores, thereby shrinking its volume. The raw pore structure could change because the gel structure in coal collapses when the moisture escapes during drying process [19]. It means that the moisture content in raw coal is not only related with microstructure characteristics, but also its absorption or desorption during coal transmission and storage before crushing can significantly affect the microstructures. Incorporating with the previous studies: Zhang et al. found that the indentation modulus of coal decreased after water absorption, and they attributed it to change of microstructure led by water adsorption [11]. Besides, Xin et al. discovered that drying coal easily leaded to changes of pore structure [12]. Thus, it can be reasonably speculated that the moisture in raw coal can also affect the microstructures and then cause changes of its mechanical and crushing properties [20]. Therefore, it is of great significance to deeply study the influence of moisture on coal mechanical properties during crushing process.

In addition, industrial coal crushing process is not an instantaneous process and the coal is actually broken by the cyclic action of external force. Under cyclic loading process, the breaking of coal is accompanied by energy dissipation, which increases steadily with the load level rising [21]. Meanwhile, as the cyclic loading times increases, the destruction of the coal microstructures becomes more severe, and the channel is formed between the pores [22, 23]. So it is of great significance to study the cumulative crushing effect of coal under cyclic loading based on evolution characteristics of microstructures. Besides, from the experiments about the effects of cyclic loading on rocks, the failure mode of the rocks under cyclic loading is very different from the failure mode under static loading. More local cracks are observed under cyclic loading process [24], and cyclic loading can cause rock cracks at lower loads [25]. Based on the micro-crack density, it is found that the damage of coal microstructures continues to increase with progress of the cycle, which results in some changes in the spatially related length [26]. In addition, in the cyclic loading experiment of artificial jointed rock, it is found that with increase of the maximum stress, the damage after circulation becomes greater and develops faster [27]. Obviously, the loading method and stress also have a significant effect on the rock crushing characteristics [24, 27]. Besides, as for coal, it can be speculated that the cyclic loading can also have significant but different effects on the mechanical properties as static loading. Further exploring the microstructures and mechanical properties of coal under cyclic loading is key to understand cumulative crushing effects.

In this work, three typical Chinese bituminous coals were chosen, the effects of moisture content and cyclic loading during coals crushing process were investigated. The images of coals surfaces and mechanical properties were recorded with a high-speed camera and a microcomputer-controlled electronic universal testing machine respectively. The roles of moisture content and cyclic loading in microstructures and their effects on mechanical properties were revealed. The evolution process of coal microstructures was quantified with the fractal dimension, and a universal relationship between microstructures and mechanical properties was finally established.

2. Experimental and methods

2.1 Experimental materials and process

Three bituminous Chinese coals (SM, HSQ, and WCW) were from Shenmu coal mine in Shaanxi province, Hongshaquan coal mine and Wucaiwan coal mine in Xinjiang province respectively. Proximate and ultimate analysis of the three raw coals are shown in our previous work [13]. Before experiments, the raw coals were uniformly cut and polished to small cube lumps (1.0 cm × 1.0 cm × 1.0 cm). Firstly, the lump coals were fully immersed in deionized water for 12 hours to achieve water-saturated, and then the water-saturated samples were placed in an oven at 120 ℃ for drying until their weights no longer decreased. In this condition, the moisture can be evaporated, and it can guarantee that its chemical structures were not destroyed [28]. Because these three coals possessed different initial moisture contents and distinct abilities to adsorb moisture, leading to the phenomenon that their moisture contents are varied at water-saturated situation. In order to compare them more accurately, the relative moisture content (RMC, %) during coal drying process was defined according to Eq. (1).

$$RMC = \frac{M - M_\infty}{M_0 - M_\infty} \times 100\% \tag{1}$$

Where M_0 (g) meant the mass of the saturated sample, M_∞ (g) was the mass of dried samples, and M (g) represented the mass of these samples at any time during drying process.

The change of relative moisture content in three coals with drying time was recorded and shown in Fig. S1. Different relative moisture contents (100%, 75%, 50%, 25%, and 0%) were selected and their corresponding drying times are shown in Table 1. Fig. 1 shows the diagram of experimental devices, and all the uniaxial load experiments were done on the microcomputer-controlled electronic universal testing machine. During the experiment, the lump coal was placed on the universal base, and then it was loaded by uniaxial load at a speed of 5 mm/min. At the same time, the microstructures on coal surface were recorded on-line with a high-speed camera at a frequency of 50 frames/second. Subsequently, SM (the raw coal) was further selected to conduct the cyclic loading experiments, because the compressive strength of SM was much larger than HSQ and WCW, suggesting SM needed more times to achieve crush, indicating that SM can be more appropriate to study the effects of cyclic loading. In order to improve the accuracy of the results, the average compressive strength for 100% stress level was measured based on five samples by uniaxial load mechanical experiments, and the results are shown in Fig. S2, from which the average compressive strength was calculated to be 16.71 MPa for 100% stress level. The other stress levels (60%, 70%, 80%, and 90%) were calculated based on 100% stress level, and they were 10.03 MPa, 11.70 MPa, 13.37 MPa, and 15.04 MPa respectively. The loading forces in constant stress and variable stress cyclic loading experiments were calculated by multiplying the cross-sectional area.

2.2 Analysis methods

In order to reflect the mechanical properties of coals uniformly, the force and displacement were recorded, and the stress (σ, MPa) and strain (ε) during uniaxial load experiments were calculated according to the following equations:

$$\sigma = \frac{F}{S_0} \tag{2}$$

$$\varepsilon = \frac{\Delta L}{L_0} \tag{3}$$

where F (N) was the force during uniaxial load, S_0 (m^2) meant the cross-sectional area, ΔL (mm) was the deformation during experiment, and L_0 (mm) represented the original height.

From the images of coal surface during uniaxial load experiments, it can be observed that the cracks develop and lump coal breaks irregularly, which are typical fractal characteristics [29]. In order to eliminate the differences between initial structures of coals, the relative stress (σ_r, MPa) and relative fractal dimension (D_r) were defined to characterize the mechanical properties and microstructures based on our previous work [13]:

$$\sigma_r = \frac{\sigma}{\sigma_{max}} \tag{4}$$

$$D_r = \frac{D - D_{min}}{D_{max} - D_{min}} \tag{5}$$

Where σ_{max} (MPa) was the maximum stress value in the experiment, σ (MPa) meant the stress value at any time, D_{max} and D_{min} were the maximum and minimum fractal dimensions, and D was the fractal dimension.

In order to better describe the cumulative process of coal crushing during cyclic loading, the strain variable was selected to quantitate the degree of crushing damage. The new strain in n-th cycle was assumed as ε_n, and in fact, the strain after n-th cycle in the stress-strain curve was the cumulative strain of n times as ε_N in Eq. (6).

$$\varepsilon_N = \Sigma(\varepsilon_n) \tag{6}$$

3. Results and discussion

3.1 Typical coal crushing process under the uniaxial load experiment

Taking raw SM for example, a typical stress-strain curve and corresponding images of the coal surface during uniaxial load experiment are shown in Fig. 2. Four stages that are compaction stage (stage A), elastic deformation stage (stage B), plasticity deformation stage (stage C), and fracture residual stage (stage D) are clearly observed respectively. From the images, it can be seen that the lump coal gradually deforms under uniaxial compression load, and new crack occurs and extends until it is broken. In stage A, the stress increases slowly, and no obvious cracks on coal surface are observed, indicating the microstructure is intact in this stage. In stage B, the stress increases continuously and the stress-strain curve is approximately a straight line, where the slope of the stress-strain curve is elastic modulus. In this stage, few cracks can be observed on the coal surface as the stress does not pass breaking limit and the structure remains unbroken. In stage C, the stress reaches and passes through the highest point (compressive strength), and obvious cracks appear on the coal surface, suggesting the lump coal microstructures suffer severe damages. Besides, the extension of the cracks leads to a rapidly drop of supporting capacity. In stage D, the stress drops sharply, new cracks continue to appear on the coal surface, and then gradually fill wholly. At this time, the lump coal is completely broken, and its initial appearance is lost.

3.2 Effects of moisture on the microstructures and mechanical properties

3.2.1 Effects of moisture on the microstructures

The relative fractal dimensions at different moisture contents during drying process of three coals are drawn in Fig. 3. As seen clearly, with the decrease of relative moisture content, the relative fractal dimension of SM does not take on an evident tendency, while the relative fractal dimensions of HSQ and WCW gradually increase. It indicates that drying process cannot significantly damage the microstructures of SM, but the cracks on HSQ and WCW surfaces gradually develop. This is because that the moisture desorption process can significantly affect the microstructures of HSQ and WCW, which improves the internal pore diameter during drying process, resulting in the production of internal force and cracks on coal surface [30]. Besides, it can be seen that the relative fractal dimensions of HSQ and WCW change rapidly when the relative moisture content decreases from 75% to 25%, revealing that the microstructures are severely damaged at this stage. The relative moisture content between 75% and 25% is a key range that should be paid attention to during the coal crushing process.

3.2.2 Effects of moisture on mechanical properties

Fig. 4 shows the relationship between compressive strength and elastic modulus for coals with different relative moisture contents. It can be seen that there is a strong positive linear relationship between the compressive strength and elastic modulus for these three coals with different relative moisture contents, whose fitted equation is as Eq. (7) and the R^2 can be as high as 0.94. Thus, this equation is suitable for these three coals with various relative moisture contents. With assists of this equation, the compressive strength can be predicted by elastic modulus that can be calculated in the initial stage B (in Fig. 2). It means the compressive strength can be predicted on the premise of keeping the lump coal unbroken, which provides a new way for efficient and quick measurement of the compressive strength of coal with different relative moisture contents.

$$Y = 42.69X + 71.18 \tag{7}$$

The compressive strengths and elastic modules of coals at different relative moisture contents are shown in Fig. 5, from which it can be seen that the change trends of the compressive strength and elastic modulus for the same coals are similar with the change of relative moisture content. The change trend is also consistent with the linear relationship between compressive strength and elastic modulus.

However, the values of compressive strengths and elastic modulus of different coals are various, and the tendencies of them with relative moisture content decreasing take on two types: (1) The compressive strength and elastic modulus of HSQ and WCW decreases as the relative moisture content decreases, and they are lowered to a minimum value when the relative moisture content is about 25%, and then increase slightly; (2) The compressive strength and elastic modulus of SM show an inverse change tendency with HSQ and WCW, they gradually increase with relative moisture content decreasing. This is because that moisture in the coals mainly possesses two effects on mechanical properties, which are strongly related with the coal porosity [30-33]: (1) High coal porosity can assist in adsorbing more moistures. Moisture desorption would cause obvious internal pore diameter improvement, thus resulting in internal force and cracks on the coal structures. In this situation, lower moisture content can lead to the phenomenon that coal is easier to be broken; (2) Low coal porosity can assist in adsorbing less moistures. Moisture adsorption would mainly play roles in softening and lubricating coal. In this situation, higher moisture content can lead to the phenomenon that coal is easier to be broken. Our previous study has shown that the porosities of HSQ, WCW and SM are 22.8%, 29.7%, and 10.8% respectively [13]. As a result of the rich porosity, the mass ratios of moisture for HSQ and WCW at saturated state are 33.05% and 38.54% respectively. While the mass ratio of moisture for SM is only 7.10% at saturated state. The evaporation of moisture could cause obvious damages on the microstructures during the drying process for HSQ and WCW, which is also consistent with the results of Fig. 3. As for SM, the drying process possesses little damage effects on the microstructures, thus the softening and lubricating effects are key to weak mechanical properties when the relative moisture content is high. Therefore, when the relative moisture content of SM is 100%, the lump coal is most easily broken. And as the relative moisture content reduces, both the softening effect and lubricating effect from moisture on the internal bedding of the coal decrease, resulting in a rise of the compressive strength and elastic modulus of the lump coal. While when the relative moisture contents of HSQ and WCW are higher, the lump coals are almost more difficult to be broken. In summary, as for coals with different porosities, the moisture of coals possesses distinct effects on their mechanical properties, which should be valued during the coal crushing process.

3.3 Effects of cyclic loading on microstructures and mechanical properties

3.3.1 Effects of cyclic loading on microstructures

As for SM (the raw coal), the changes of relative fractal dimension with cyclic loading times increasing under constant and variable stresses cyclic loading are exhibited in Fig. 6. As a whole, under the initial cycles, the surface does not change, but the internal structures are damaged gradually, which causes the further change of the surface microstructures under the next action. As the number of cycles reaches a certain amount, the internal structures changes accumulated to a critical point, and the microstructures evolve rapidly. However, the detailed break processes and characteristics under constant and variable stresses are different.

Taking 70% stress level for example (Fig. 6 (a)), it can be found that the change of the relative fractal dimension can be divided into four stages during the constant cyclic loading process. Firstly, the relative fractal dimension remains basically unchanged in the first four cyclic loads, following which the relative fractal dimension increases significantly under the 5th load. Then the relative fractal dimension at 6-8th cyclic loads does not change significantly. The relative fractal dimensions both increase significantly after 9th and 10th loads, and the coal structures are destroyed. It indicates that the microstructures become more complicated as damage degree deepens. During this process, new cracks continuously generate and gradually penetrate, and they change greatly in the later stage of cyclic loading. After the last cyclic load, the work effects by external force change from quantitative to qualitative. The coal structures are destroyed, and the lump coal is thus broken.

During the variable stress cyclic loading experiments, the relative fractal dimension also changes with the increase of cyclic times (Fig. 6 (b)), revealing that the coal microstructures change obviously with the increase of cyclic times. At 60% and 70% stress levels, when the cyclic times increases, the relative fractal dimension only changes slightly, indicating that the load mainly produces elastic deformation at this process, and the microstructures have not been destroyed. When the stress level increases to 80%, the relative fractal dimension increases significantly from 0.05 to 0.71, suggesting that 80% stress level can produce obvious effects on the increase of its fractal dimension [34]. At this stage, the lump coal has obvious plastic deformation, and the changes of coal microstructures are significantly obvious. Then the microstructures continue to change under 90% stress load until the lump coal is finally broken.

3.3.2 Effects of cyclic loading on mechanical properties

In order to explore the corresponding changes in mechanical characteristics of lump coals during cyclic loading process, taking 70% stress level for example, the stress-strain curve is shown in Fig. S3. It can be clearly seen that during the constant stress cyclic loading, a stress-strain hysteresis curve generates in each cycle. Besides, with increase of cycles, new strains gradually generate, and the stress-strain hysteresis curve gradually shifts to the right. After the last cyclic load, the lump coal is broken. The cumulative work has reached the energy required for coal break, indicating that the coal crushing process is gradually cumulative. Besides, the strain accumulation and cyclic load times under constant stress of SM at 70% stress level are shown in Fig. S4. It shows that during the cyclic loading process, the cumulative amount of strain gradually increases as the number of cycles continuously increases, which indicates that the effect of loading on coal gradually deepens. When the lump coal is broken, the strain accumulation reaches the maximum value. Meanwhile, the changes of microstructures for SM are obvious after the 5th, 9th, and 10th cycles, it is consistent with the results in Fig. 6 (a) that the strain accumulation of SM also increases more significantly after 5th, 9th, and 10th cycles, which also proves that greater increase in strain would lead to more obvious changes of the microstructures in the coal surface.

In the process of variable stresses cyclic loading (from 60% stress level to 100% stress level) for the raw SM coal, the strain accumulation can quantitatively describe the crushing degree, and the results are shown in Fig. 7. During the cyclic loading of the same stress levels, the strain accumulation increases slowly with the increase of cycle times. However, when the cyclic load stress level increases, the strain accumulation would increase significantly. The cumulative effect of strain shows a step-up state, which indicates that the increased force process possesses a significant effect on the coal destruction.

Fig. 8 shows the average proportion of strain generated by 25 cycles of SM1-SM4. It can be seen that first cyclic load can produce the largest strain proportion (72.05%). In addition, the load of first cyclic time after increase of stress level is also significantly greater than those of 2-5 cyclic times. Except for the first load of each stress level (1st, 6th, 11th, 16th, and 21th times), the remaining 20 loads account for a small proportion of the strain with an average proportion of 0.36%. These results directly show that the effect of cyclic loading under constant force on coal is far less than the effect of gradual increased force, suggesting that the coal crushing process with a gradual increased stress level is preferred.

3.4 Relationship between microstructures and mechanical properties

Previous researches have shown that mechanical properties are strongly related with the microstructures of coals during crushing process [35, 36]. However, no universal relationship has been built yet. Thus, in order to build the universal relationship between coal microstructures and mechanical properties during coal crushing process, the experimental data of the relative fractal dimensions and relative stresses are fitted in Fig. 9, and quantitative relationship can be expressed as Eq. (8), for which the R^2 can be as high as 0.85.

$$\sigma_r = -0.67D_r^2 + 1.62D_r + 0.07 \tag{8}$$

As a whole, it can be obviously seen that as the relative fractal dimension increases, the relative stress shows an upward trend, and the trend is universally applicable for the three coals with various relative moisture contents. So the mechanical properties can be acquired by the relative fractal dimensions of coal surface images, and the relative error is expected to be very small. Besides, in the variable stresses cyclic loading experiments of SM, the relative fractal dimension with the change of relative stress can also fit to the relationship interestingly. Furthermore, the quantitative relationship excludes the effect of these three Chinese bituminous coals under different moisture contents and cyclic loading through two dimensionless parameters of relative fractal dimension and relative stress, and only focuses on the relationship between the microstructures and mechanical properties during coal crushing process. It reveals that the association between microstructures and mechanical properties, indicating that mechanical properties of coal could be predicted by its surface images, which is extremely important and significant to guide coal grinding crushing.

4. Conclusions

Taking typical Chinese bituminous coals as research objectives, the roles of moisture and cyclic loading in microstructures and their effects on mechanical properties were detailedly investigated, and main conclusions can be drawn as follows:

(1) The effects of moisture on the mechanical properties for the coals strongly depended on porosity. For low porosity coal (SM), moisture mainly softened and lubricated, thus reducing the compressive strength and elastic modulus. For high porosity coal (HSQ and WCW), moisture desorption process would create some cracks and fractures, thus reducing compressive strength and elastic modulus.

(2) Under the cyclic loading process, the cumulative effect of strain showed a step-up state under different stress levels. The first load in the cyclic loading produced the largest strain, and caused the most obvious damage on coal structures.

(3) The mechanical properties of raw coals were strongly related with their microstructures. There was a normalized quantitative relationship between the relative stress and relative fractal dimension during coal crushing, which can be expressed as $\sigma_r = -0.67D_r^2 + 1.62D_r + 0.07$.

Acknowledge

This work was financially supported by the National Natural Science Foundation of China (No. 51576072, No. 51806073, No. 21908156, U1910214). The authors also acknowledge the extended help from Analytical and Testing Center of Huazhong University of Science and Technology.

References

[1] BP Energy Outlook, 2019. https://www.bp.com/en/global/corporate/energy-economics/energy-outlook.html.

[2] Xu J., Tang H., Su S., Liu J., Xu K., Qian K., et al. A study of the relationships between coal structures and combustion characteristics: The insights from micro-Raman spectroscopy based on 32 kinds of Chinese coals. Applied Energy 2018; 212: 46-56. https://doi.org/10.1016/j.apenergy.2017.11.094.

[3] Zhou W., Wang H., Wang D., Zhang K., Du Y., Yang H.. The effect of geometries and cutting parameters of conical pick on the characteristics of dust generation: Experimental investigation and theoretical exploration. Fuel Processing Technology 2020; 198: 106243. https://doi.org/10.1016/j.fuproc.2019.106243.

[4] He Y., Xie W., Zhao Y., Li H., Wang S.. Triboelectrostatic separation of pulverized fuel of coal power plant based on mineralogical analyses. International Journal of Mineral Processing 2017; 166: 7-12. https://doi.org/10.1016/j.minpro.2017.06.005.

[5] Xie W., He Y., Yang Y., Shi F., Huang Y., Li H., et al. Experimental investigation of breakage and energy consumption characteristics of mixtures of different components in vertical spindle pulverizer. Fuel 2017; 190: 208-220. https://doi.org/10.1016/j.fuel.2016.11.026.

[6] Sung Y., Moon C., Eom S., Choi G., Kim D.. Coal-particle size effects on NO reduction and burnout characteristics with air-staged combustion in a pulverized coal-fired furnace. Fuel 2016; 182: 558-567. https://doi.org/10.1016/j.fuel.2016.05.122.

[7] Pan R., Qiu T., Chao J., Ma H., Wang J., Li C.. Thermal evolution of the oxidation

characteristics of pulverized coal with different particle sizes and heating rates. Thermochimica Acta 2020; 685: 178516. https://doi.org/10.1016/j.tca.2020.178516.

[8] Liu X., Tan Y., Ning J., Lu Y., Gu Q.. Mechanical properties and damage constitutive model of coal in coal-rock combined body. International Journal of Rock Mechanics and Mining Sciences 2018; 110: 140-150. https://doi.org/10.1016/j.ijrmms.2018.07.020.

[9] Dong J., Cheng Y., Hu B., Hao C., Tu Q., Liu Z.. Experimental study of the mechanical properties of intact and tectonic coal via compression of a single particle. Powder Technology 2018; 325: 412-419. https://doi.org/10.1016/j.powtec.2017.11.029.

[10] Chen S., Yin D., Jiang N., Wang F., Zhao Z.. Mechanical properties of oil shale-coal composite samples. International Journal of Rock Mechanics and Mining Sciences 2019; 123: 104120. https://doi.org/10.1016/j.ijrmms.2019.104120.

[11] Zhang Y., Lebedev M., Al-Yaseri A., Yu H., Xu X., Sarmadivaleh M., et al. Nanoscale rock mechanical property changes in heterogeneous coal after water adsorption. Fuel 2018; 218: 23-32. https://doi.org/10.1016/j.fuel.2018.01.006.

[12] Xin F., Xu H., Tang D., Cao L.. An improved method to determine accurate porosity of low-rank coals by nuclear magnetic resonance. Fuel Processing Technology 2020; 205: 106435. https://doi.org/10.1016/j.fuproc.2020.106435.

[13] Shan L., Hu S., Zhang Y., Wu P., Xu K., Xu J., et al. Relationship between fractal meso-structural and mechanical characteristics of lump coal under uniaxial compression at different temperatures. Fuel Processing Technology 2019; 194: 106112. https://doi.org/10.1016/j.fuproc.2019.05.035.

[14] Yu H., Zhang Y., Lebedev M., Han T., Verrall M., Wang Z., et al. Nanoscale

geomechanical properties of Western Australian coal. Journal of Petroleum Science and Engineering 2018; 162: 736-746. https://doi.org/10.1016/j.petrol.2017.11.001.

[15] Xu J., Liu J., Zhang X., Ling P., Xu K., He L., et al. Chemical imaging of coal in micro-scale with Raman mapping technology. Fuel 2020; 264: 116826. https://doi.org/10.1016/j.fuel.2019.116826.

[16] Li Y., Yang J., Pan Z., Tong W.. Nanoscale pore structure and mechanical property analysis of coal: An insight combining AFM and SEM images. Fuel 2020; 260: 116352. https://doi.org/10.1016/j.fuel.2019.116352.

[17] Hu S., Shan L., Xu B., Su J., Wang Y., Jiang L., et al. Meso-mechanical properties evolution during fracture of coal cubes under loading. Journal of China Coal Society 2018; 43: 855-861. https://doi.org/10.13225/j.cnki.jccs.2017.0970.

[18] Charrière D., Behra P.. Water sorption on coals. Journal of Colloid and Interface Science. 2010; 344: 460-467. https://doi.org/10.1016/j.jcis.2009.11.064.

[19] Yu J., Tahmasebi A., Han Y., Yin F., Li X.. A review on water in low rank coals: The existence, interaction with coal structure and effects on coal utilization. Fuel Processing Technology 2013; 106: 9-20. https://doi.org/10.1016/j.fuproc.2012.09.051.

[20] Zhang Q., Fan X., Chen P., Ma T., Zeng F.. Geomechanical behaviors of shale after water absorption considering the combined effect of anisotropy and hydration. Engineering Geology 2020; 269: 105547. https://doi.org/10.1016/j.enggeo.2020.105547.

[21] Song D., Wang E., Liu J.. Relationship between EMR and dissipated energy of coal rock mass during cyclic loading process. Safety Science 2012; 50: 751-760. https://doi.org/10.1016/j.ssci.2011.08.039.

[22] Jiang C., Duan M., Yin G., Wang J., Lu T., Xu J., et al. Experimental study on seepage properties, AE characteristics and energy dissipation of coal under tiered cyclic loading. Engineering Geology 2017; 221: 114-123. https://doi.org/10.1016/j.enggeo.2017.03.005.

[23] Pan R., Ma Z., Yu M., Chao J., Li C., Wang J.. Study on the mechanism of coal oxidation under stress disturbance. Fuel 2020; 275: 117901. https://doi.org/10.1016/j.fuel.2020.117901.

[24] Geranmayeh Vaneghi R., Ferdosi B., Okoth A., Kuek B.. Strength degradation of sandstone and granodiorite under uniaxial cyclic loading. Journal of Rock Mechanics and Geotechnical Engineering 2018; 10: 117-126. https://doi.org/10.1016/j.jrmge.2017.09.005.

[25] Erarslan N.. Microstructural investigation of subcritical crack propagation and Fracture Process Zone (FPZ) by the reduction of rock fracture toughness under cyclic loading. Engineering Geology 2016; 208: 181-190. https://doi.org/10.1016/j.enggeo.2016.04.035.

[26] Zhang Z., Wang E., Li N., Li X., Wang X., Li Z.. Damage evolution analysis of coal samples under cyclic loading based on single-link cluster method. Journal of Applied Geophysics 2018; 152: 56-64. https://doi.org/10.1016/j.jappgeo.2018.03.014.

[27] Liu M., Liu E.. Dynamic mechanical properties of artificial jointed rock samples subjected to cyclic triaxial loading. International Journal of Rock Mechanics and Mining Sciences 2017; 98: 54-66. https://doi.org/10.1016/j.ijrmms.2017.07.005.

[28] Feng L., Yuan C., Mao L., Yan C., Jiang X., Liu J., et al. Water occurrence in lignite and its interaction with coal structure. Fuel 2018; 219: 288-295. https://doi.org/10.1016/j.fuel.2018.01.097.

[29] Zhou S., Liu D., Cai Y., Yao Y.. Fractal characterization of pore-fracture in low-rank coals

using a low-field NMR relaxation method. Fuel 2016; 181: 218-226. https://doi.org/10.1016/j.fuel.2016.04.119.

[30] Yang X., Jiang Y., Shao X.. Drying intensity affected to pore structure and water re-adsorption in lignite. Coal Science and Technology 2014; 42: 109-112. https://doi.org/10.13199/j.cnki.cst.2014.04.028.

[31] Sampath K., Perera M., Li D., Ranjith P., Matthai S.. Evaluation of the mechanical behaviour of brine+CO_2 saturated brown coal under mono-cyclic uni-axial compression. Engineering Geology 2019; 263: 105312. https://doi.org/10.1016/j.enggeo.2019.105312.

[32] Zhang X., Ranjith P., Lu Y., Ranathunga A.. Experimental investigation of the influence of CO2 and water adsorption on mechanics of coal under confining pressure. International Journal of Coal Geology 2019; 209: 117-129. https://doi.org/10.1016/j.coal.2019.04.004.

[33] Zhong C., Zhang Z., Ranjith P., Lu Y., Choi X.. The role of pore water plays in coal under uniaxial cyclic loading. Engineering Geology 2019; 257: 105125. https://doi.org/10.1016/j.enggeo.2019.05.002.

[34] Yu B., Chen Z., Wu J.. Experimental study on compaction and fractal characteristics of saturated broken rocks with different initial gradations. Journal of Mining & Safety Engineering 2016; 33: 342-347. https://doi.org/10.13545/j.cnki.jmse.2016.02.024.

[35] Hu S., Su J., Xu B., Shan L.. Surface structure evolution of coal cubes during compression process and its relationship with mechanical properties. Huazhong Univ. of Sci & Tech. (Natural Science Edition) 2017; 45: 118-122. https://doi.org/10.13245/j.hust.170122.

[36] Xu H., Wang G., Fan C., Liu X., Wu M.. Grain-scale reconstruction and simulation of coal mechanical deformation and failure behaviors using combined SEM Digital Rock data and

DEM simulator. Powder Technology. 2020; 360: 1305-1320. https://doi.org/10.1016/j.powtec.2019.07.014.

Tables

Table 1 Drying time of relative moisture content for the three coals (min)

RMC	100%	75%	50%	25%	0%
SM	0	34	80	150	300
HSQ	0	17	52	110	300
WCW	0	13	43	95	300

Figures

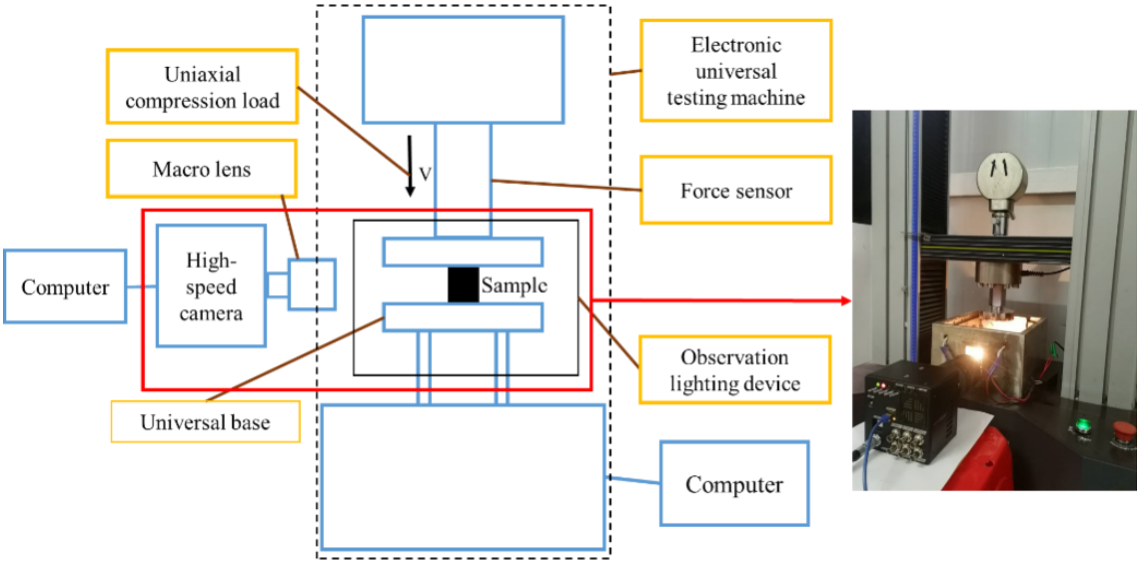

Fig. 1. Diagram of experimental devices

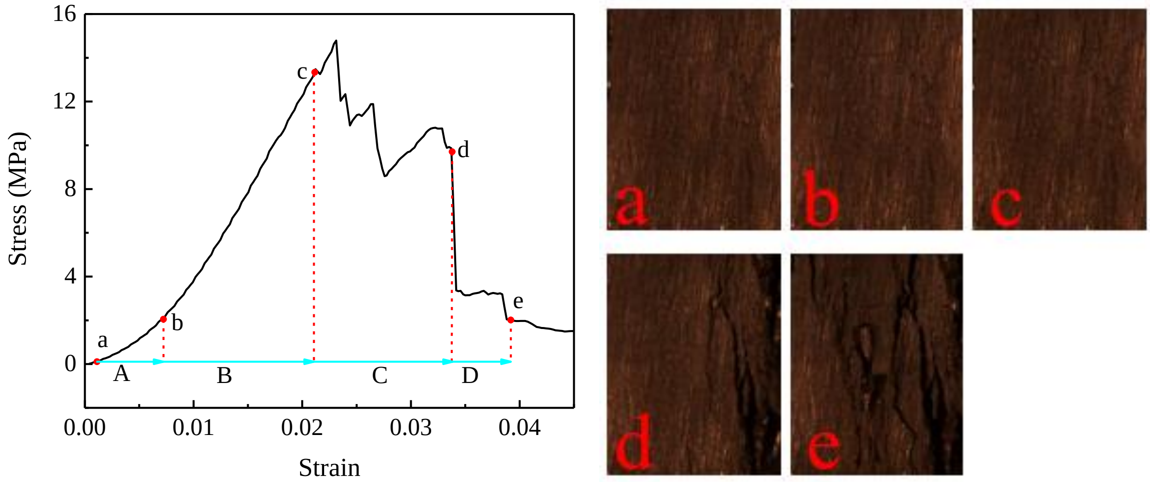

Fig. 2. Typical stress points and corresponding coal surface images for SM

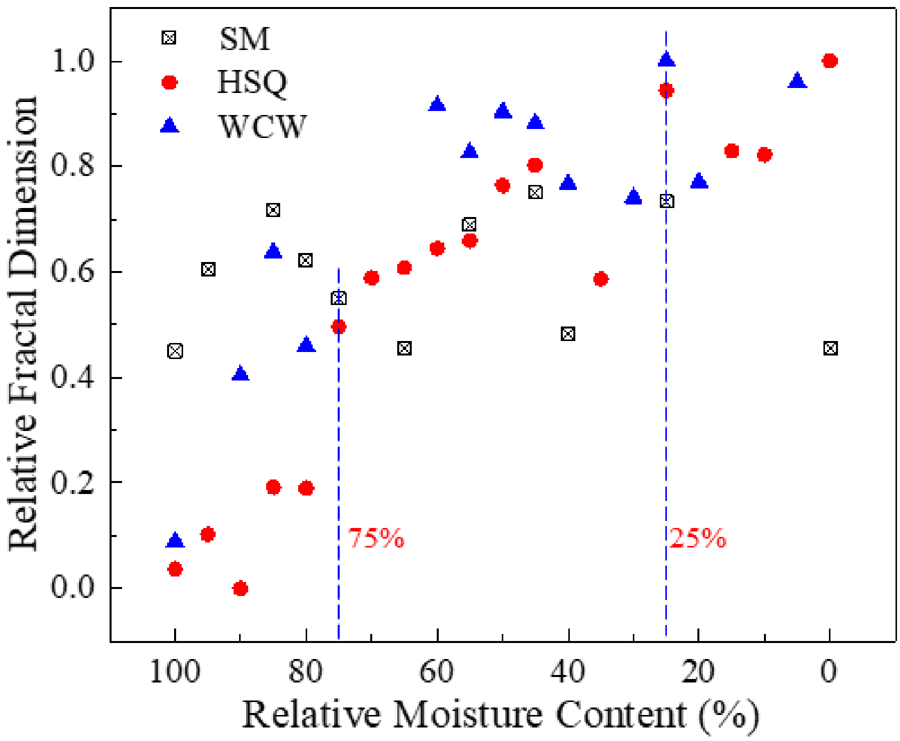

Fig. 3. The relative fractal dimension at different moisture contents during drying process of three coals

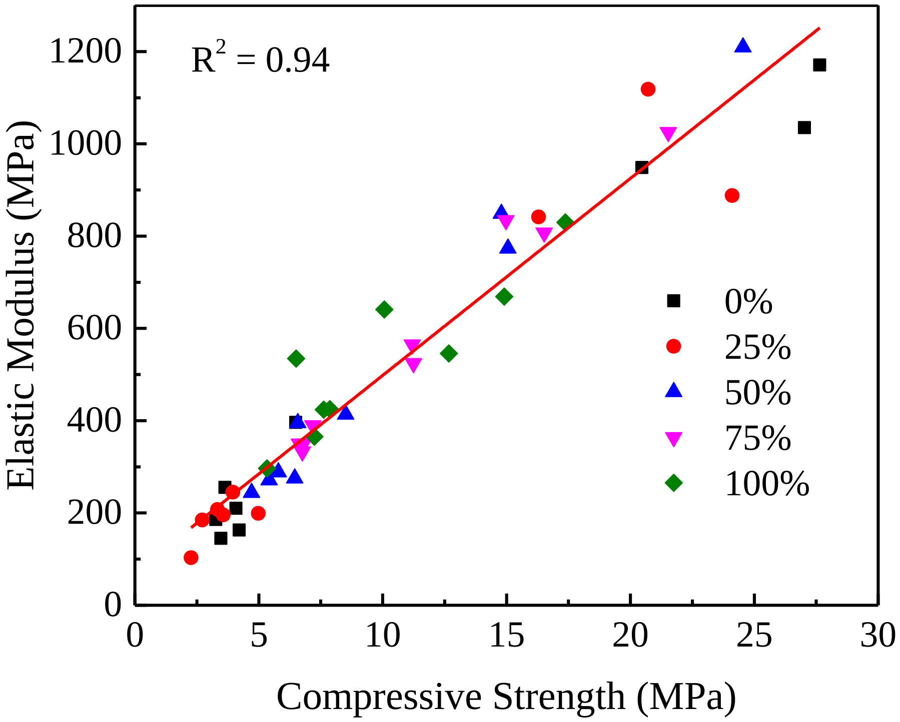

Fig. 4. Relationship between compressive strength and elastic modulus for coals with different relative moisture contents

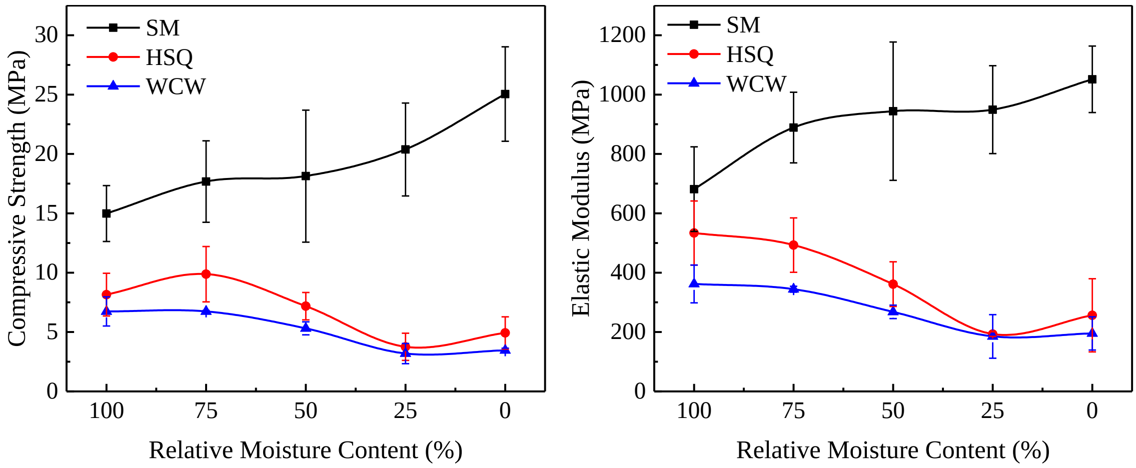

Fig. 5. Compressive strength and elastic modulus of three coals with different moisture contents

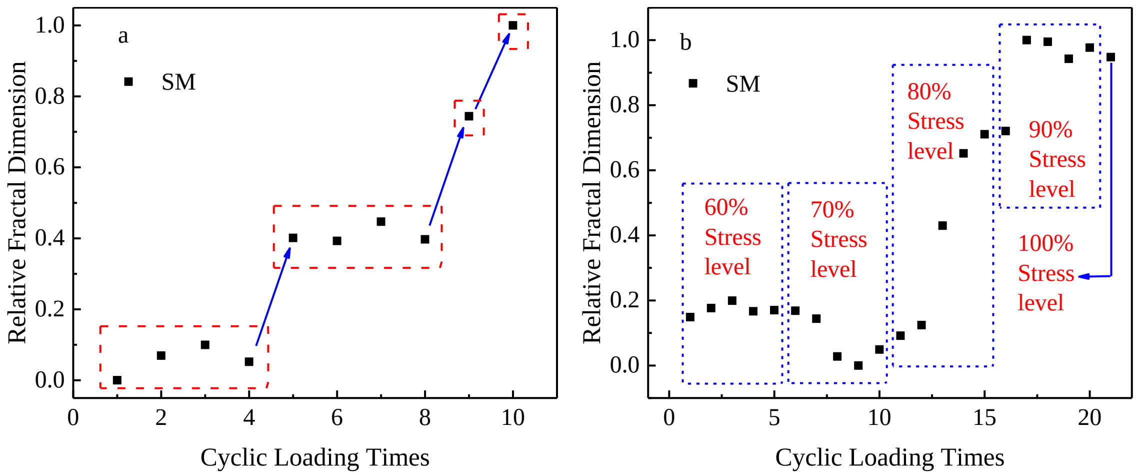

Fig. 6. Microstructures evolution of SM: (a) Under constant stress cyclic loading (70% stress level), (b) Under variable stress cyclic loading

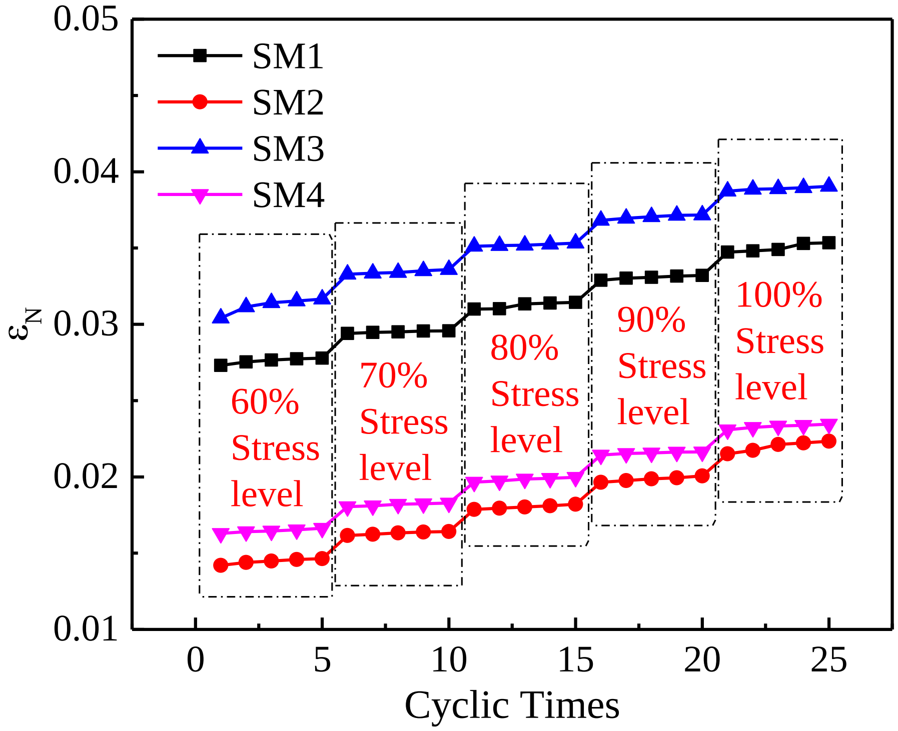

Fig. 7. Strain accumulation under cyclic loading with variable stress

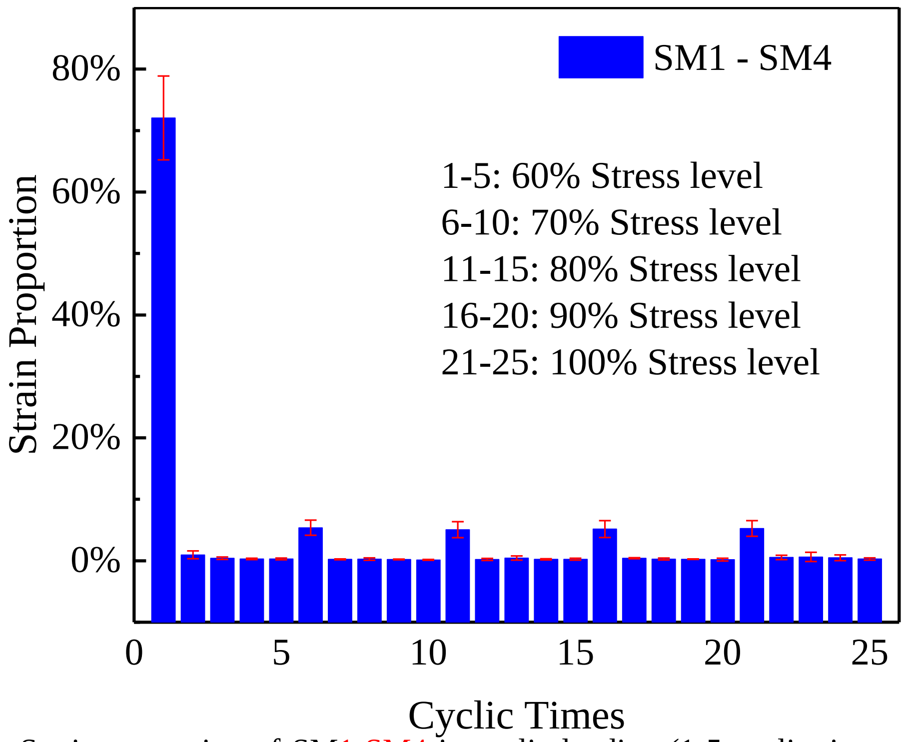

Fig. 8. Strain proportion of SM1-SM4 in cyclic loading (1-5 cyclic times: 60% stress level, 6-10 cyclic times: 70% stress level, 11-15 cyclic times: 80% stress level, 16-20 cyclic times: 90% stress level, 21-25 cyclic times: 100% stress level)

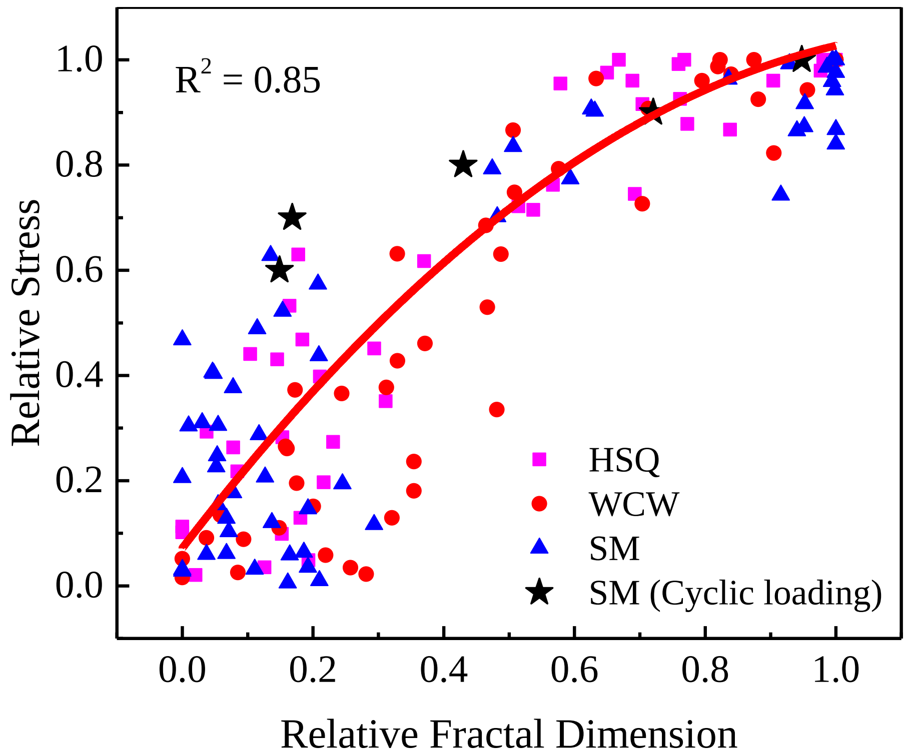

Fig. 9. Relationship between relative fractal dimension and relative stress of three coals